ChemComm

COMMUNICATION

View Article Online
View Journal | View Issue

Check for updates

Cite this: *Chem. Commun.*, 2020, **56**, 4102

Received 7th February 2020,
Accepted 9th March 2020

DOI: 10.1039/d0cc00990c

rsc.li/chemcomm

Published on 09 March 2020. Downloaded by Universiteit Twente on 6/24/2021 9:44:06 AM.

The role of water and influence of hydrogen bonding on the self-assembly aggregation induced emission of an anthracene-guanidine-derivative†

Pedro J. Pacheco-Liñán, ‡[a] Cristina Martín,‡[bc] Carlos Alonso-Moreno,[cd] Alberto Juan,[ef] Daniel Hermida-Merino,[g] Andrés Garzón-Ruíz,[a] José Albaladejo,[h] Mark Van der Auweraer,[b] Boiko Cohen *[i] and Iván Bravo *[ac]

We report a luminescent anthracene-guanidine derivative that forms rare T-shape dimers, resulting in an excimer with a quantum yield approaching one. Water plays a fundamental role through H-bonding guiding the self-assembly. These results establish a new framework for environmentally friendly aggregation-induced emission luminogens.

Over the years the need for novel luminescent materials has dramatically increased to fulfill the demand of a wide variety of fields such as nanotechnology, electronic molecular materials or sensors.[1] Although phosphors can be employed as emitters (normally based on rare-earth elements) their toxicity or scarce availability, as well as the low emission quantum efficiency, especially in the presence of water, brought forward the need for alternative luminescent materials.[2] π-Conjugated molecules or polymers have been suggested as potential candidates to produce luminescent materials based on their high synthetic flexibility, easy purification and low cost.[1] One of the main disadvantages of these systems is the aggregation caused emission quenching (ACEQ) in the solid state due to formation of non-emissive aggregates (*e.g.* π–π stacking leading to H-aggregates).[3] One solution to mitigate the ACEQ is the design of novel molecules that feature aggregation induced emission (AIE).[4,5] Although the mechanism behind the AIE is not well-established, two fundamental parameters have been frequently identified: (a) restriction of the intramolecular motions and (b) reduction of the π–π stacking interactions and/or modification of the symmetry of the aggregates from H-type to J-type.[6] Thus, the structure–properties relationship of the core and the side groups of the new materials showing AIE (AIEgens) should be properly selected to ensure the reduction of both the molecular motions and the π–π stacking interactions, using these two factors as design guidelines.

Anthracene derivatives have been widely investigated as core structure for AIEgens due to their excellent luminescent behavior and high stability.[7] However, the aggregation induces only weak emission in comparison to the monomer in solution.[8] Several studies have shown that H-type π–π stacking of the anthracene can be reduced by tuning the size of the side groups in such a way that the self-assembled orientation is controlled through steric hindrance by the functional groups.[9–11] The use of hydrogen-bonding groups (like amines or amides) is poorly explored, even though they could reinforce the molecular rigidity and at the same time prevent the non-desired aggregations by proton transfer processes. Of all H-bonding groups, the guanidine moiety gives one of the most stable complexes as its chemical structure allows to stabilize the net charge.[12,13]

Taking into account the overlooked properties of the guanidine moiety,[13,14] a new anthracene-guanidine AIEgen: 2-(anthracen-1-yl)-1,3-diisopropylguanidine (1GA) was synthetized following an atom-economical hydroamination of carbodiimides (guanylation reaction, see the ESI† for further details).[12] This work demonstrates, for the first time, that the inclusion of this functional group gives rise to exceptional photophysical properties due to a guidance of the self-assembly by H-bonding interactions with water molecules.

The absorption spectra of 1GA (Fig. 1a) in toluene is characterized by two bands, one at 350 nm with vibronic structure typical for

[a] Departamento de Química Física, Facultad de Farmacia de Albacete, Universidad de Castilla-La Mancha, Albacete-02071, Spain. E-mail: ivan.bravo@uclm.es
[b] Molecular Imaging and Photonics, Department of Chemistry, Katholieke Universiteit Leuven, Celestijnenlaan 200F, 3001 Leuven, Belgium
[c] Unidad de Medicina Molecular, Centro Regional de Investigaciones Biomédicas, Albacete, Spain
[d] Departamento de Inorgánica, Orgánica y Bioquímica, Facultad de Farmacia de Albacete, UCLM, Albacete-02071, Spain
[e] Department of Biomolecular Nanotechnology, MESA+ Institute for Nanotechnology and TechMed Institute for Health and Biomedical Technologies, Faculty of Science and Technology, University of Twente, P.O. Box 217, 7500 AE, Enschede, The Netherlands
[f] Department of Molecular NanoFabrication, MESA+ Institute for Nanotechnology, Faculty of Science and Technology, University of Twente, P.O. Box 217, 7500 AE, Enschede, The Netherlands
[g] Netherlands Organization for Scientific Research, DUBBLE at the ESRF, 71 Avenue des Martyrs, CS40220, 38043 Greno-ble, France
[h] Instituto de Investigación en Combustión y Contaminación Atmosférica, Universidad de Castilla-La Mancha, Camino de Moledores s/n, Ciudad Real, 13071, Spain
[i] Departamento de Química Física, Facultad de Ciencias Ambientales y Bioquímica, and INAMOL, Universidad de Casti-lla-La Mancha, Avenida Carlos III, S/N, 45071 Toledo, Spain. E-mail: boyko.koen@uclm.es

† Electronic supplementary information (ESI) available. See DOI: 10.1039/d0cc00990c
‡ These authors contributed equally.

This journal is © The Royal Society of Chemistry 2020

Published on 09 March 2020. Downloaded by Universiteit Twente on 6/24/2021 9:44:06 AM.

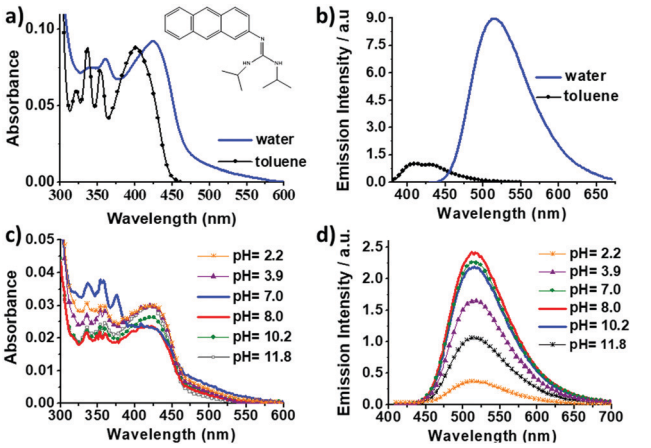

Fig. 1 Absorption (a) and emission (b) spectra of 1GA in water and toluene (10 μM). Absorption (c) and emission (d) spectra of 1GA in aqueous solution at different pH values (10 μM). The inset shows the chemical structure of the AIEgen 1GA. The excitation wavelength for the emission spectra is 350 nm.

anthracene and its derivatives,[15] and a second, non-structured band at 400 nm. Similar spectral behavior has been reported for other anthracene amino derivatives, such as 1- and 2-aminoanthracene, where the 350 nm band is assigned to a $\pi \rightarrow \pi^*$ transition of the $S_0 \rightarrow S_n$ (^1L_a) and the 400 nm is attributed to a charge transfer (CT) process.[16] The emission spectrum of 1GA in toluene (Fig. 1b), following excitation at 350 nm, has a maximum of intensity at 410 nm (full width at half maximum, FWHM = 4600 cm^{-1}, fluorescence quantum yield, ϕ = 0.27), which partially preserves the vibronic structure of the anthracene moiety. In spite of the loss of vibronic structure, the Stokes shift remains relatively modest (610 cm^{-1}). This suggests a notable change in the equilibrium geometry of 1GA due to a possible torsional movement of the guanidine moiety, which is more significant in the excited state. Similar behavior has been reported for other anthracene derivatives, where the substitution by an ester group produces different distorted structures in the excited state.[17]

In water, at pH 7.0, the 350 nm band partially preserves its vibronic structure and undergoes a modest red shift. The band at 400 nm however shifts to 426 nm, corresponding to a red shift of 1530 cm^{-1}. Additionally, a red-edge tail is observed in the aqueous solution, which is most probably due to light scattering by aggregates (*vide infra*). The emission spectrum of 1GA in water at pH 7.0 (Fig. 1b), following excitation at 350 nm, consists of a structureless band with a maximum at 510 nm, corresponding to a Stokes shift of 3870 cm^{-1}. The spectral behavior of 1GA is accompanied by a significant increase in ϕ from 0.27 in toluene to 0.72 in water. The increased Stokes shift and loss of fine structure of the emission spectrum in water could be due to the CT character of the excited state. However, the large increase of the Stokes shift cannot be explained only by the increase in polarity. This suggests a larger conformational change upon excitation of 1GA when in aqueous solution, which is related to the guanidine substitution, where the ability of H-bonding interaction with water molecules results in a more rigid structures and potentially formation of aggregates (giving rise to the AIE phenomena). The protonation of the guanidine group in aqueous solutions, as reported for other guanidine derivatives or 1-aminoanthracene,[18] can play an important role in the formation of a more rigid system. This is further supported by the increase in the fluorescence lifetime 11 ± 1 ns in toluene and 25 ± 2 ns in water, (pH 7.0) and by the ~3 fold enhancement in the quantum yield in water.

In order to unravel the exact photoluminescence mechanism of 1GA, the pH dependence of its steady-state and time-resolved behavior was studied. While in the absorption spectra (Fig. 1c), only small differences are observed over a broad range of pH values, the emission (Fig. 1d) intensity is enhanced by a factor of 8 when the pH increases from 2.2 to 8.0. Notably, this emission enhancement is not accompanied by a shift of the emission maximum (~515 nm) or a change in the width of the emission band (~3280 cm^{-1}). Upon further increase of the pH, the emission intensity decreases again by more than a factor of two at pH 11.8. The emission transients (Fig. 2a) recorded following excitation at 360 nm and collected at 495 nm are mono-exponential (mean fluorescence decay time, τ_m = 25 ns) and unaffected by the pH (pH 2.2 and pH 10.2). At pH 11.8, a notable decrease in the value of τ_m is observed and it becomes 14 ns, similar to 11 ns obtained in toluene. While at high pH the decrease of τ_m matches the decrease of the fluorescence intensity, this is not the case for pH between 2.2 and 8.0. In this range the change in the pH affects the equilibrium between the emissive and non-emissive species characterized by similar absorption spectrum (Fig. 2a). Thus, although the pH is not modifying the existing 1GA ground state species, it is an important parameter for its emission properties and therefore for the AIE mechanism.

Next, we consider different scenarios for the AIE mechanism, the first one being the presence of excited state intermolecular proton transfer (ESPT), in similarity with other molecules having the guanidine entity in their molecular structure, such as the naphthalene derivative.[14] To evaluate this scenario, the kinetic isotopic effect (KIE) was explored by comparing the excited state dynamics of 1GA in D_2O to that in water (Fig. 2b).

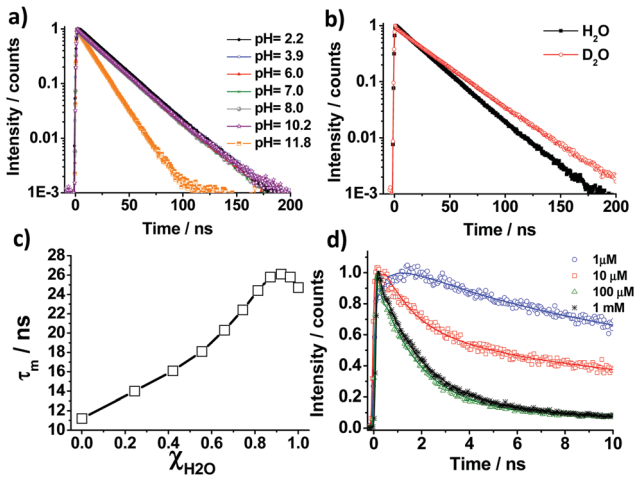

Fig. 2 (a) Fluorescence intensity decays of 1GA in aqueous solutions at different pH values; (b) excited-state dynamics of 1GA in water and deuterated water; (c) average fluorescence lifetimes of 1GA in ACN in presence of varying water content (χ_{H_2O}); (d) concentration dependence of the excited state dynamics of 1GA in aqueous solution at pH 7.0. λ_{exc} = 360 nm and λ_{obs} = 495 nm.

Published on 09 March 2020. Downloaded by Universiteit Twente on 6/24/2021 9:44:06 AM.

In these conditions τ_m changes from 25 ns in water to 30 ± 3 ns in D_2O giving rise to a KIE of 1.2. This value, along with the lack of the geminate recombination signature in the emission decay, as evidenced by the mono-exponential transients, suggest lack of ESPT in the 1GA system.[19,20] Another explanation for the observed pH dependence is the self-assembly of 1GA in dimers or larger aggregates stabilized through H-bond interactions between the water molecules and 1GA. This aggregation and H-bond formation can result in a more rigid 1GA molecular conformation and reduce the rate constant of the non-radiative decay. To get insight into this possibility, the formation of water assisted H-bonded-1GA dimers was studied by observing the excited state behavior of 1GA in mixtures of an aprotic solvent (acetonitrile, ACN) and water, with varying water molar fraction (χ_{H_2O}) (Fig. 2c). The change in the intensity of the emission spectra and the quantum yields of the 1GA ACN : H_2O mixtures upon excitation at 360 nm (Fig. 2S, ESI†) indicates an enhancement of the radiative process upon increasing the water concentration until a maximum is reached at χ_{H_2O} = 0.9, where the fluorescence quantum yield approaches unity. The fluorescence decays of 1GA in the ACN : H_2O mixtures are bi-exponential (Table S3, ESI†) and τ_m gradually changes from 11 ns in pure ACN (χ_{H_2O} = 0), which corresponds to the lifetime of the 1GA monomer (as observed for toluene, 11 ns), to a maximum of ∼25 ns at 60% (weight) water content (χ_{H_2O} = 0.9). The value of τ_m at χ_{H_2O} = 0.9 along with the steady-state spectra agree with the previously reported T-shaped geometry of anthracene dimers in anthracene-containing polyamidoamine dendrimer.[21,22] Unusual T-shaped geometry for anthracene has also been reported for other anthracene derivatives, where the presence of water results in a dimer formation at the ground state, which in turn leads to the same type of structure in the excited state.[23–27] To verify the role of the water molecules in the formation of the H-bonded 1GA dimers with T-shaped geometry, and at the same time to exclude the effect of proton transfer and hydrogen bond formation in absence of water, the excited state dynamics of 1GA in ACN in presence of varying amounts of trifluoroacetic acid (TFA) was also studied (ESI,† Table S2). Although the observed fluorescence decays were not mono-exponential, τ_m = 11 ns independent of the TFA concentration. This suggests that the proton transfer does not play an important role in the AIE mechanism. Thus, the intramolecular H-bond interactions in the 1GA dimer through water molecules are a key factor in the AIE process. Upon excitation this dimer relaxes to a T-shape excimer, which accounts for the AIE behavior. It should be noted that we do not exclude the possibility that the ground state dimer is already in the T-shape-like configuration.

A Job Plot allows to assess the number of water molecules involved in the formation of the T-shaped excimer.[28,29] Fig. 2c shows an asymmetrical dependence of τ_m in ACN/H_2O on the water content with a maximum observed around χ_{H_2O} = 0.9, which corresponds to 3 molecules of water per guanidine derivate. Similar results were observed for other supramolecular systems forming an A_3B complexes.[28,29] On the other hand, above this χ_{H_2O} the value of τ_m decreases again probably due to formation of aggregates with a different packing, thus demonstrating the importance of the exact water concentration for the formation of the highly-emissive T-shaped excimers.

Bearing in mind that the 1GA : water ratio in ACN : H_2O mixtures is crucial for the formation of the ground state dimers giving rise to the AIE, one can expect that the concentration of 1GA will also affect the photophysics of 1GA. Fig. 3S (ESI†) depicts the effect of 1GA concentration on the excitation and emission spectra. At high concentrations a red-edge shoulder related to the non-desired π–π stacking shows up in the excitation spectrum (∼450 nm), whereas the emission spectrum is blue shifted, as it was previously observed for anthracene aggregates.[11] At low 1GA concentration (1 μM) the decay of the 495 nm emission transient attributed to the T-shaped excimer (λ_{exc} = 360 nm) is characterized by a rise with a time constant of 690 ps followed by an almost mono-exponential decay with τ_m = 22 ns, characteristic for the T-shaped excimer. The rising component suggests a major conformational change of the dimer after excitation. Upon increasing the 1GA concentration (>100 μM), the rising component is not observed while the decay becomes multi-exponential with τ_m = 14 ± 1 ns (∼2 times shorter than the one of the excited T-shaped dimer). Fig. 4S (ESI†) shows the concentration dependence of the obtained lifetime amplitudes. The long component (∼25 ns) has its maximum contribution when the 1GA concentration is below 10 μM (independently of the observation wavelength) and its contribution significantly decreases at higher concentrations (>10 μM). On the other hand, the shortest component (1–4 ns) becomes the dominant one at higher concentrations and is negligible at 1 μM. This suggests that upon increasing the 1GA concentration it preferentially forms π–π stacking aggregates which undergo significant conformational relaxation after excitation leading to a suppression of the T-shaped excimer formation.[30]

To confirm the formation of the T-shaped dimers in aqueous solution, DFT calculations (Fig. 3) and SAXS experiments were performed. The SAXS experiments undoubtedly demonstrate the existence of aggregates/dimers in the ground state with an estimated size of about 1.5 nm using a sphere-fitting model (Fig. 5S, ESI†). This value is in agreement with the most stable dimer obtained by the DFT calculations. In this structure, one water molecule acts as a bridge between two 1GA monomers. This complex is surrounded by two additional water molecules, most probably next to the two guanidine moieties to stabilize the total charge. According to the calculation the HOMO and LUMO are located on two different anthracenes molecules. Hence the HOMO to LUMO transition of the dimer corresponds to the population of a state with CT character (Fig. 3a). This indicates that the CT character of the formed dimer is another key factor in the AIE mechanism. A recent study has reported on the synthesis and photophysical characterization of anthracene-guanidine derivative with substitution at 9th position. In this study the authors observed an increase in the emission intensity in strongly alkaline aqueous solutions but did not observe evidence for excimer formation. The different behavior can be explained by the lack of CT character of the resulting anthracene-guanidine derivative, which is evidenced by the absence of the characteristic CT band in the absorption spectrum at 400–420 nm.[31] Excited-state calculations for the excimer

 This journal is © The Royal Society of Chemistry 2020

Published on 09 March 2020. Downloaded by Universiteit Twente on 6/24/2021 9:44:06 AM.

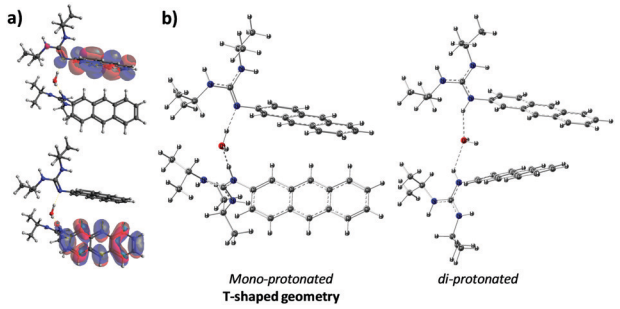

Fig. 3 (a) HOMO (up) and LUMO (down) molecular orbitals at B3LYP/6-31+G* level of theory. (b) Optimized geometries of mono and deprotonated dimers in water at B3LYP/6-31+G* level Conclusions.

emission in the anthracene dimer in the crystal of 2-(anthracen-9-yl)-thianthrene (2-TA-AN) have indicated a stabilization by mixing the CT and the LE states which gives rise to the observed excimer emission.[32] This stabilization leads to an increase in the overall rigidity of the excimer structure, resulting in a significant suppression of the non-radiative energy deactivation by restricting the intermolecular vibrations and rotations in the excimer skeleton. When co-planar dimer structure in solid state is considered, such as the case of 2-TA-AN, the interaction between the two anthracene entities occurs through shortening of the inter-planar π–π distance and increasing of the inter-monomer π–π overlap at the excimer equilibrium geometry. However, for the 1GA T-shape dimer, the water molecules play a crucial role into the overall process of excimer formation as, on one hand they serve as a relay between the two monomers, while on the other hand, they stabilize the geometry that favors the orbital interaction that stabilizes the excimer yielding the 500 nm emission. Another important observation from the DFT calculations is that the dimeric structure has to be mono-protonated for the formation of the T-shaped conformation, supporting the pH dependence of the steady-state emission (Fig. 1d). Thus, at high pH values (above the pK_a of 1GA), 1GA is in the non-protonated form while at low pHs it is di-protonated resulting, in both cases, to less extensive formation of T-shaped dimers in the ground state.

In conclusion, a new AIEgen has been obtained (QY ∼ 1) based on the formation of a dimer in the ground state assisted by up to 3 water molecules, which leads to highly emissive T-shaped excimer. The experimental results along with theoretical calculations prove that the inclusion of guanidine group at the correct position is crucial to open a new framework for developing more environmentally friendly AIEgen molecules.

We acknowledge financial support from MINECO, Spain (Grant No. CTQ2017-84131-R and CTQ2016-81797-REDC Programa Redes Consolider). This work was also supported by the Research Foundation-Flanders (FWO, grant no. G.0B39.15 and G098319N); FWO postdoctoral fellowships to C. M. (grant no. 12J1719N and 12J1716N), the KU Leuven Re-search Fund (C14/15/053); the Flemish government through long-term structural funding Methusalem (CASAS2, Meth/15/04); the Hercules Foundation (HER/11/14); and the Belgian Federal Science Policy Office (IAP-VII/05). BC acknowledges support from JCCM, Spain, grant no. SBPLY/19/180501/000212.

Conflicts of interest

There are no conflicts to declare.

Notes and references

1 A. Kitai, *Luminescent Materials and Applications*, John Wiley & Sons, 2008, vol. 25.
2 Y. Li, M. Gecevicius and J. L. Qiu, *Chem. Soc. Rev.*, 2016, **45**, 2090.
3 T. Förster and K. Kasper, Ein Konzentrationsumschlag Der Fluoreszenz Des Pyrens, *Zeitschrift für Elektrochemie, Berichte der Bunsengesellschaft für physikalische Chemie*, 1955, **59**, 976.
4 Y. Hong, J. W. Y. Lam and B. Z. Tang, *Chem. Soc. Rev.*, 2011, **40**, 5361.
5 J. Mei, N. L. C. Leung, R. T. K. Kwok, J. W. Y. Lam and B. Z. Tang, *Chem. Rev.*, 2015, **115**, 11718.
6 Y. Chen, J. W. Y. Lam, R. T. K. Kwok, B. Liu and B. Z. Tang, *Mater. Horiz.*, 2019, **6**, 428.
7 Q. Li and Z. Li, *Adv. Sci.*, 2017, **4**, 1600484.
8 J. Huang, J.-H. Su and H. Tian, *J. Mater. Chem.*, 2012, **22**, 10977.
9 H. Liu, L. Yao, B. Li, X. Chen, Y. Gao, S. Zhang, W. Li, P. Lu, B. Yang and Y. Ma, *Chem. Commun.*, 2016, **52**, 7356.
10 Y. Shen, H. Liu, S. Zhang, Y. Gao, B. Li, Y. Yan, Y. Hu, L. Zhao and B. Yang, *J. Mater. Chem. C*, 2017, **5**, 10061.
11 C. Zhao, X. Cai, Z. Ma, J. Shi, L. Xu and H. Wang, *J. Photochem. Photobiol., A*, 2018, **355**, 318.
12 C. Alonso-Moreno, A. Antiñolo, F. Carrillo-Hermosilla and A. Otero, *Chem. Soc. Rev.*, 2014, **43**, 3406.
13 K. A. Schug and W. Lindner, *Chem. Rev.*, 2005, **105**, 67.
14 P. J. Pacheco-Liñán, J. Fernández-Sainz, I. Bravo, A. Garzón-Ruiz, C. Alonso-Moreno, F. Carrillo-Hermosilla, A. Antiñolo and J. Albaladejo, *J. Phys. Chem. C*, 2018, **122**, 9363.
15 J. Van Damme and F. Du Prez, *Prog. Polym. Sci.*, 2018, **82**, 92.
16 S. G. Schulman, R. M. Threatte, A. C. Capomacchia and W. L. Paul, *Asian J. Pharm. Sci.*, 1974, **63**, 876.
17 M. A. Omary and H. H. Patterson, in *Encyclopedia of Spectroscopy and Spectrometry*, ed. J. C. Lindon, Academic Press, Oxford, 2nd edn, 1999, p. 1194.
18 S. Watanabe, K.-I. Kumagai, M. Hasegawa, M. Kobayashi, J. Okubo, T. Yoshinaga, H. Hiratsuka and T. Hoshi, *Bull. Chem. Soc. Jpn.*, 2000, **73**, 1783.
19 D. Huppert and E. Pines, *Methods of Laser Spectroscopy*, Springer, 1986, p. 113.
20 E. Pines and D. Huppert, *J. Phys. Chem.*, 1983, **87**, 4471.
21 G. Zhang, G. Yang, S. Wang, Q. Chen and J. S. Ma, *Chem. – Eur. J.*, 2007, **13**, 3630.
22 P. K. Lekha and E. Prasad, *Chem. – Eur. J.*, 2010, **16**, 3699.
23 S. Hisamatsu, H. Masu, M. Takahashi, K. Kishikawa and S. Kohmoto, *Cryst. Growth Des.*, 2015, **15**, 2291.
24 P. F. Jones and M. Nicol, *J. Phys. Chem.*, 1968, **48**, 5440.
25 L. B. Clark and M. R. Philpott, *J. Phys. Chem.*, 1970, **53**, 3790.
26 G. Biesmans, G. Verbeek, B. Verschuere, M. Van der Au'weraer and F. De, *Thin Solid Films*, 1989, **169**, 142.
27 W. S. Durfee, W. Storck, F. Willig and M. D. Von Frieling, *J. Am. Chem. Soc.*, 1987, **109**, 1297.
28 J. S. Renny, L. L. Tomasevich, E. H. Tallmadge and D. B. Collum, *Angew. Chem., Int. Ed.*, 2013, **52**, 11998.
29 N. L. Truex and J. S. Nowick, *J. Am. Chem. Soc.*, 2016, **138**, 13891–13900.
30 T. Hinoue, Y. Shigenoi, M. Sugino, Y. Mizobe, I. Hisaki, M. Miyata and N. Tohnai, *Chem. – Eur. J.*, 2012, **18**, 4634.
31 K. Heemoon, L. Hyun Koo, C. Sung and K. Hyung Jin, *J. Photochem. Photobiol., A*, 2019, **383**, 112023.
32 Y. Gao, H. Liu, S. Zhang, Q. Gu, Y. Shen, Y. Ge and B. Yang, *Phys. Chem. Chem. Phys.*, 2018, **20**, 12129.